Carbohydrate Polymers 95 (2013) 716–727

Contents lists available at SciVerse ScienceDirect

Carbohydrate Polymers

journal homepage: www.elsevier.com/locate/carbpol

Coelectrospinning of chitosan/alginate fibers by dual-jet system for modulating material surfaces

Wei-Wen Hu*, Hsing-Ning Yu

Department of Chemical and Materials Engineering, National Central University, Jhongli City, Taiwan

ARTICLE INFO

Article history:
Received 13 November 2012
Received in revised form 15 February 2013
Accepted 27 February 2013
Available online 26 March 2013

Keywords:
Alginate
Chitosan
Electrospinning
Surface modification
Degradation
Composite

ABSTRACT

Chitosan and alginate are two frequently used biomaterials for tissue engineering. In this study, electrospinning technique was applied for their nanofiber fabrications to mimic extracellular environment (ECM). Polyethylene oxide (PEO) was applied to increase viscosities of polymer solutions to obtain nanofibers with appropriate morphologies. To modulate surface properties, a dual jet system was developed to coelectrospin chitosan and alginate nanofibers on one substrate. Because the deposition rates of electrospun fibers linearly correlated to the perfusion rates of polymer solutions, the composition ratios of nanofibers were thus manipulated, which determined both the chemical properties and hydrophobicity of fibrous mats. *In vitro* cell culture results suggested that the cell morphology highly depended on the fiber composition, and the composite nanofibers demonstrated higher biocompatibility than that on pure fibers. Finally, the degradation of alginate fibers was controlled by the crosslinking process. Reducing calcium ions resulted in partial fiber degradation, by which the composition ratios of nanofibers varied with time. This dynamically changed environment performed a promising property to improve viability of surface cells. Through this tunable system, surface properties of scaffolds can be finely adjusted to benefit tissue engineering applications.

1. Introduction

Biomaterials play important roles in tissue engineering because they provide an appropriate environment to mimic extracellular matrix (ECM). Polysaccharides are attractive biomaterials because they are easily found in different organisms and are biocompatible. Among them, alginate and chitosan are two frequently used polysaccharides for biomedical applications, which are derived from brown seaweed and crustacean shells, respectively.

Alginate is an anionic polysaccharide material. Divalent cations, such as Ca^{2+}, can be used to crosslink alginate for gelation. Alginate has been broadly used for chondrocyte adhesion because of its D-glucuronic acid residue which is similar to hyaluronic acid structure (Dar, Shachar, Leor, & Cohen, 2002). In addition, alginate is a hydrophilic material which can maintain water to create an ECM-like aqueous environment. However, the low protein adsorption of alginate makes it difficult to interact with cells *via* cell surface receptors (Rowley, Madlambayan, & Mooney, 1999). Therefore, various methods have been studied to overcome this drawback. For example, RGD-sequence has been applied to modify alginate for improving cell adhesion (Jeon, Powell, Ahmed, & Alsberg, 2010).

The combination of chitosan and alginate provides an alternative approach. Compared to anionic alginate, amine groups of chitosan offer a positive-charged surface. In addition, chitosan is a relative hydrophobic material, and thus can promote protein adsorption and cell adhesion. Alginate-based chitosan hybrid polymer fibers have been prepared by the wet-spinning method, which demonstrate an improved adhesion capacity with rabbit tendon fibroblast and annulus fibrous cells compared to pure alginate polymer fiber (Majima et al., 2005; Shao & Hunter, 2007). However, these wet-spinning fibers are micron scale, which have fewer surfaces for cell adhesion than that of natural ECM. In contrast, electrospinning technique provides an easy strategy to fabricate continuous nanofibers from different ranges of polymers, which can not only decrease material defects to promote mechanical strength, but also increase surface area for cell adhesion (Sill & von Recum, 2008). Both chitosan and alginate have been applied to electrospin nanofibers (Bhattarai, Edmondson, Veiseh, Matsen, & Zhang, 2005; Bhattarai, Li, Edmondson, & Zhang, 2006; Geng, Kwon, & Jang, 2005; Lu, Zhu, Guo, Hu, & Yu, 2006). However, the combination of chitosan and alginate solutions for electrospinning is a challenge because these two polymers complex quickly through the electrostatic interaction, and the formed gel may block the needle to inhibit the polymer jet. Alternative approaches are to prepare these two polymers as core/sheath fibers or deposit on the

* Corresponding author at: Department of Chemical and Materials Engineering, National Central University, No. 300 Jhongda Road, Jhongli City, Taoyuan County, Taiwan. Tel.: +886 3 422 7151x34243; fax: +886 3 422 5258.
E-mail address: huweiwen@cc.ncu.edu.tw (W.-W. Hu).

0144-8617/$ – see front matter © 2013 Elsevier Ltd. All rights reserved.
http://dx.doi.org/10.1016/j.carbpol.2013.02.083

other nanofibers as layer-by-layered form; however, only one of the material can be exposed at the outer layer (Chang, Lee, Wu, Yang, & Chien, 2012; Deng et al., 2011; Ritcharoen, Supaphol, & Pavasant, 2008). *In situ* mixing of these two polymer solutions before electrospinning has been studied, whereas the blending ratio is limited due to material compatibility. For example, the mixtures of high chitosan or high alginate blending ratios always lead to bead-containing nanofibers (Jeong et al., 2011). Therefore, to obtain chitosan/alginate nanofibers with arbitrary ratios, we developed a dual jet system in this study. Chitosan and alginate solutions were electrospun separately using two independent power supply system. The morphologies of electrospun nanofibers were regulated by adding PEO to polymer solutions. The deposition ratios of two nanofibers were controllable by adjusting their perfusion rates. This method provided an easy and feasible way to modulate surface properties through altering the composition ratios of composite fibers.

Furthermore, the porosity of scaffolds may highly affect seeded cells. For example, the pore sizes of scaffolds is critical to osteogenesis (Karageorgiou & Kaplan, 2005). The control of fiber sizes of scaffolds has also been studied to regulate cell differentiation and infiltration (Woodfield et al., 2005). For electrospinning, the porosity and pore sizes can be easily controlled by altering the fiber sizes, deposition rates, the styles of collector, postelectrospinning modification, or selectively removal of partial fibers (Baker et al., 2008; Nam, Huang, Agarwal, & Lannutti, 2007; Rnjak-Kovacina et al., 2011; Soliman et al., 2010; Telemeco et al., 2005; Vaquette & Cooper-White, 2011). In this study, because the stability of alginate structure relies on the crosslinking of calcium ions, the removal of alginate can be regulated by changing the crosslinking condition. It should be able to provide a dynamically changed matrix environment to manipulate cell adhesion and infiltration.

2. Materials and methods

2.1. Materials

Chitosan with molecular weight of 50–190 kDa, sodium alginate with molecular weight of 80–120 kDa, and polyethylene oxide (PEO) with molecular weight of 900 kDa were purchased from Sigma–Aldrich. Dulbecco's modified Eagle medium (D-MEM), fetal bovine serum (FBS), and trypsin–EDTA were obtained from Gibco.

2.2. Preparation of chitosan and alginate solutions

Chitosan was dissolved in 40% acetic acid to make a final concentration of 9 wt.% as stock solution. Sodium alginate and PEO were dissolved in water with concentrations of 6 and 10 wt.%, respectively. It took 1–3 days at 60 °C before complete solution was achieved. Before electrospinning, chitosan/PEO or alginate/PEO solutions were prepared with different ratios, and residual part was supplemented by surfactant Triton X-100 as well as cosolvent dimethyl sulfoxide (DMSO) in water that the final concentrations of Triton X-100 and DMSO were 0.5% and 10%, respectively. The mixtures were stirred overnight and centrifuged to remove air bubbles before use.

2.3. Viscosities of polymer solutions

MCR 501 rheometer (Anton-Paar, Austria) was utilized to determine the shear viscosities of chitosan/PEO or alginate/PEO solutions. The shear rates ranging from 0.1 to 10 s^{-1} were applied during viscosity examination, and the viscosities at the shear rate of 1 s^{-1} was used to determine the viscosity effect on electrospinning.

2.4. Electrospinning of nanofibers

In order to deposit two different nanofibers on one substrate, we designed a dual electrospinning system which was shown in Supplementary Fig. s1. The polymer solutions were fed into two 1 ml disposable syringes with 24G needle tips (inner diameter = 0.29 mm) which were connected to two separate power supplies (Chargemaster CH50-P, Simco) with identical voltages of 15 kV. Glass cover slips with diameters of 16 mm were placed on a grounded stainless steel plate to collect electrospun fiber. The distances between tips and the collector were 20 cm for all tests. To avoid the interference between jets of chitosan/PEO and alginate/PEO solutions, there was a switch to control two power supplies that each polymer solution jetted for 15 s in turn. Neat chitosan/PEO or alginate/PEO nanofibers were prepared by single nozzle electrospinning, using the same conditions as the dual jet system with the flow rate of 2 μl/min. The spun nanofibers were dried in an oven at 37 °C for 1 day.

2.5. Scanning electron microscopy (SEM)

Nanofibers were sputter coated with gold and their morphologies were illustrated by scanning electron microscopy (SEM, 3500N, Hitachi, Japan). The diameters of nanofibers were evaluated by 100 measurements based on their SEM images. To analyze the collection rates at different feed rates, chitosan/PEO or alginate/PEO solutions were electrospun to glass substrate for 5 min. The lengths of nanofiber in SEM images were analyzed by software (NIS Elements Basic Research, Nikon, Japan), which were divided by the area of the whole images to determine the fiber density.

2.6. Fluorescence staining of nanofibers

To distinguish the distribution of different nanofibers on substrates, fluorescein and rhodamine B were used to label chitosan/PEO and alginate/PEO solutions, respectively. These dyes were dissolved in water with concentrations of 1 wt.%, and 10 μl of stain solutions were added to 5 ml of polymer solutions. The electrospinning was performed for 5 min, and the collected nanofibers were observed using fluorescent microscopy (Eclipse Ti-U, Nikon, Japan).

2.7. X-ray photon–electron spectrometry (XPS)

Nanofibers were deposited for 2 h to cover slips, and these fibrous mats were dried in vacuum oven at 37 °C overnight. Chemical analysis of electrospun fibers was performed by X-ray photon-electron spectrometry (XPS, K-alpha, Thermo, USA) to evaluate the element composition of surface fibers.

2.8. Fourier transform infrared (FTIR) spectroscopy

Chitosan, alginate, and composite nanofibers were electrospun for 2 h. These fibrous mats were examined by FTIR (FT/IR 410, Jasco, USA) with a resolution of 4 cm^{-1} between 4000 and 600 cm^{-1}.

2.9. Contact angle analysis

Water contact angle of electrospun nanofibers was determined by Drop Shape Analysis system (DSA10, Kruss GmbH, Hamburg, Germany). Four measurements per substrate were taken and the data were demonstrated as averages with standard deviations.

2.10. Cell morphology experiments

Human embryonic kidney cell line (HEK-293T) (ATCC, Manassas, VA, USA) was used to evaluate biocompatibility of nanofibers. These cells were cultured in DMEM containing 10% FBS and were incubated at 37 °C with 5% CO_2.

Nanofibers were deposited to circular glass cover slips for 1.5 h before cell seeding. These electrospun nanofibers were immersed in 99.5% ethanol solutions with 2% $CaCl_2$ for 2 h and were rinsed with PBS thrice before placing in 24-well multiplates. On the other hand, chitosan and alginate films were fabrication as the control groups. Chitosan and alginate was dissolved in 0.35 M acetic acid and ddH_2O, respectively, for the final concentrations of 0.5 wt.%. Two hundred microliters of polymer solutions were added in 24-well multiplates before placing in 37 °C oven overnight for solvent evaporation. These films were also treated by 99.5% ethanol solutions with 2% $CaCl_2$ and following PBS washes before cell culture experiments.

Finally, HEK-293T cells were seeded at density of 5000 cells per well, and the cell morphologies were analyzed by inverted microscope (Eclipse Ti-U, Nikon, Japan).

2.11. Biocompatibility of nanofibers

To evaluate biocompatibility of nanofibers, HEK 293T cells were seeded to electrospun mats or films placed in 24-well multiplate at density of 20,000 cells per well. Lactate dehydrogenase (LDH) and (4,5-cimethylthiazol-2-yl)-2,5-diphenyl tetrazolium bromide (MTT) assays were performed to quantify the cell numbers and cell viability, respectively.

The LDH assay for cell number quantification was determined by CytoTox 96 non-radioactive cytotoxicity assay (Promega, Madison, WI, USA) according to kit instruction for total cell number assay. Briefly, 0.5 ml of fresh medium was replaced in each well before the assay, and 75 μl of lysis buffer was added to sample for 1 h at 37 °C to release LDH from live cells. Then, 50 μl of these medium were moved to 96-well multiplates to react with 50 μl of LDH reagent for 30 min at room temperature. Finally, 50 μl of stop solution was added to each well and was analyzed spectrophotometrically at a wavelength of 490 nm. Additionally, there was a standard curve made by lysing known cell amounts to convert absorbance to total cell number.

For the MTT assay, 100 μl of MTT solution (5 mg/ml in PBS) was added to nanofiber sample with 900 μl of medium for 3 h at 37 °C. The supernatant was removed and 1 ml of DMSO was added to dissolve formazan from cells, which was analyzed spectrophotometrically at a wavelength of 550 nm.

3. Results

3.1. Electrospinning of chitosan nanofibers

Chitosan has been prepared in acetic acid solutions for electrospinning because concentrated acetic acid can not only increase solubility of chitosan but also reduce surface tension of solution to enhance the efficiency of electrospinning (Geng et al., 2005). However, amine groups of chitosan become positive charged in acidic condition that their repulsive forces may inhibit the formation of continuous fiber, especially during the jet stretching (Min et al., 2004). Hydrophilic PEO has been applied to reduce defect of chitosan nanofibers because of hydrogen bonds formation between oxygen of PEO and amines of chitosan, which can break down the inter- and intrachain interactions of chitosan (Bhattarai et al., 2005). Additionally, the present of PEO can increase solution chain entanglements, which can reduce bead formation during electrospinning (Duan, Dong, Yuan, & Yao, 2004). To comprehensively determine appropriate ranges for electrospinning, polymer solutions with different ratios of chitosan and PEO were prepared in this study. Triton-X 100 and DMSO were added as surfactant and cosolvent to increase the compatibility between chitosan and PEO (Bhattarai et al., 2005).

The morphologies of electrospun fibers were characterized by SEM (Fig. 1a). Pure chitosan solutions had been used for electrospinning; however, beads and incomplete fibers were formed that ideal nanofiber formation were unavailable (data not shown). For chitosan solutions with 1 wt.% of PEO (P1), nanofibers were able to be formed when chitosan was 3 wt.% (C3P1), although some beads were found during deposition. Complete nanofiber could be spun when chitosan concentrations were higher than 3 wt.%, suggesting that high concentration of chitosan can improve nanofiber formation. For 2 wt.% of PEO (P2), the threshold of chitosan solution was decreased to 2 wt.%. For PEO with 3 wt.% or more, all concentrations of chitosan can be applied to electrospinning. These results demonstrated that either increasing chitosan or PEO concentrations can efficiently reduce defects of nanofibers.

The SEM images were also used to measure the diameters of electrospun nanofibers. The size of nanofibers increased with increasing chitosan concentrations (Fig. 1b). Similar trends were also found by changing PEO concentrations, whereas the enlargement efficiencies of PEO to nanofibers were more obvious than that of chitosan (Fig. 1c).

Because electrospinning is highly affected by viscosity, rheometry was applied to measure the viscosities of different polymer solutions at the shear rate of 1 s^{-1} (Supplementary Table s1a). These results suggested that viscosities increased with the polymer concentrations. The correlation between viscosities and the corresponding diameters suggested that greater viscosities of polymer solutions spun nanofibers with larger diameters (Supplementary Fig. s2a). It should be due to that increasing viscosity retarded the flow ability of polymer jet, which eventually enlarged the diameter of electrospun fiber. Additionally, the concentration effects on fiber diameters may also be contributed by their higher solid contents. In contrast, solutions which cannot successfully electrospin nanofiber was due to their low viscosities. Only solutions with viscosities lager than 2.07 Pa s (C2P2) could be applied to electrospinning.

3.2. Electrospinning of alginate nanofibers

Electrospinning of alginate is a challenge because gelation of alginate solution may occur even at a very low concentration, whereas reducing concentrations of alginate may result in insufficient polymer chains to achieve enough interchain entanglement for complete fiber formation. The incorporation of PEO has been applied to increase the entanglement between polymer chains to facilitate fiber formation (Bhattarai et al., 2006; Lu et al., 2006). Therefore, similar to chitosan, different concentrations of PEO and alginate were applied to determine appropriate composition of polymer solution for electrospinning. Surfactant Triton X-100 and DMSO were also used to increase the polymer solubility in this study.

Pure alginate solutions without PEO could not form complete fiber (data not shown). When PEO was 1 wt.%, complete nanofiber structure was available with 4 wt.% of alginate (A4P1). However, polymer solution was too sticky when alginate was 5 wt.% (A5P1), which made polymer jet incapable of being formed for spinning. The threshold of alginate concentration was reduced to 3 wt.% when PEO was 1.5 and 2 wt.%, suggesting that PEO increased entanglement. When PEO was 2.5 wt.%, nanofibers could be spun even alginate was at concentration of 1 wt.%. Similar to alginate, too high concentrations of PEO also inhibited polymer jet formation and hence the electrospinnings of A1P7 was unavailable. The diameter

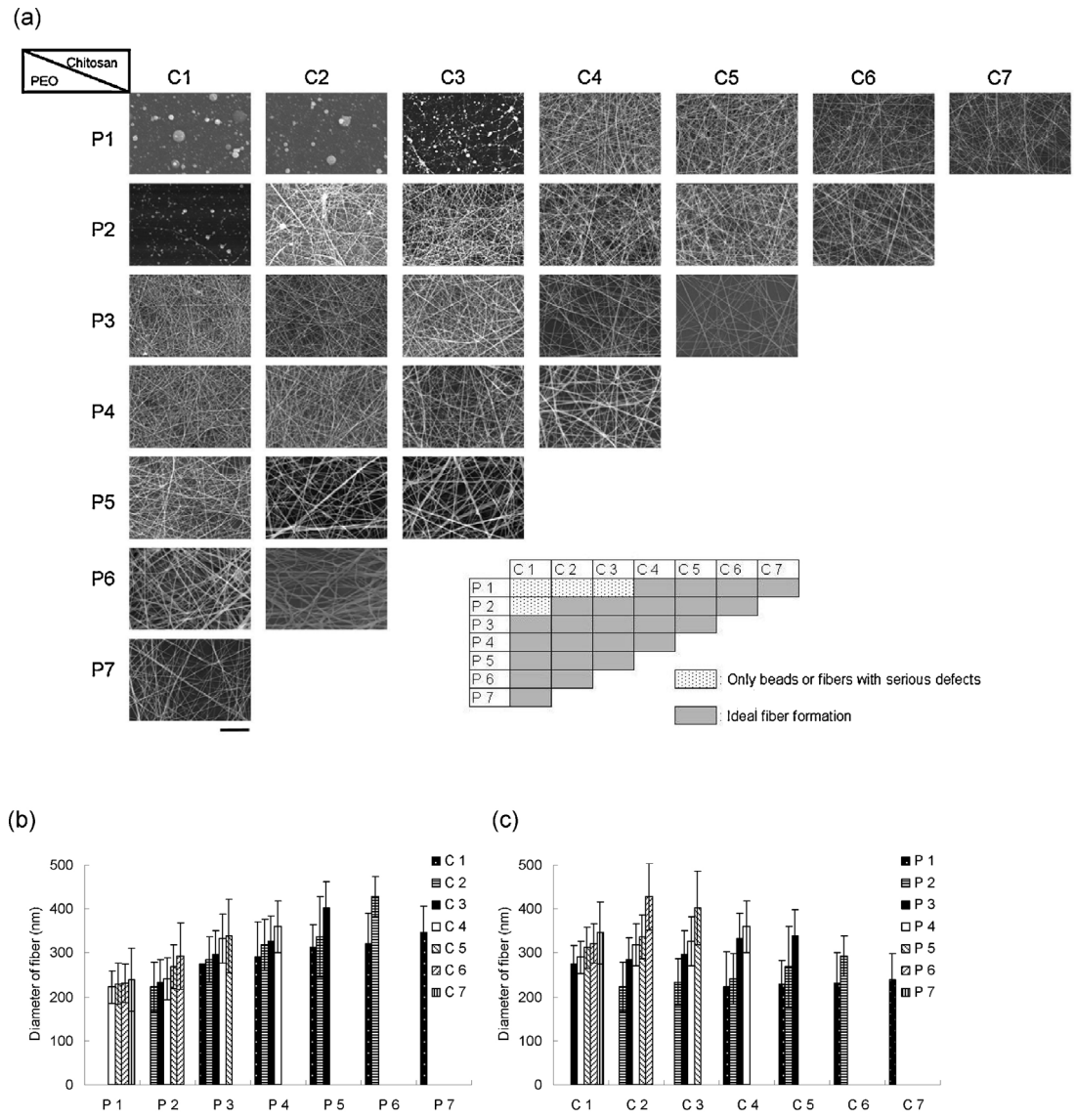

Fig. 1. The electrospinning of chitosan/PEO fibers. (a) Polymer solutions with different concentrations of chitosan and PEO were used for electrospinning, and the appropriate concentration range was also determined (scale bar = 10 μm). The diameters of nanofibers were compared using polymer solutions with different concentrations of (b) chitosan and (c) PEO.

distribution suggested that increasing concentrations of alginate or PEO can enlarge nanofibers (Fig. 2b and c). Rheometry demonstrated that increasing either alginate or PEO can increase the viscosities of polymer solutions (Supplementary Fig. s2b). Similar to chitosan nanofibers, the higher viscosities of alginate/PEO solutions resulted in larger fiber formation. The viscosities of A1P2, A2P1.5, and A2P2 were 2.97, 5.04, and 7.11 Pa s, respectively (Supplementary Table s1b). These results suggested that polymer solutions with low viscosities were unable to provide enough entanglement between polymer chains, and thus only beads or non-ideal fiber were formed in these groups. In contrast, the viscosities of A5P1 and A1P7 were 53.8 and 70.0 Pa s, respectively. These polymer solutions should be too viscous to flow in needles for fiber formation.

3.3. Preparation of composite chitosan/alginate nanofibers

According to previous experiments, C6P2 and A4P2.5 were applied for electrospinning in the following study because they have appropriate morphologies (Figs. 1a and 2a). The diameters of C6P2 and A4P2.5 were 293 ± 46 and 322 ± 52 nm, respectively (Figs. 1b and 2b).

In order to determine the electrospinning efficiencies of these two polymer fibers, both C6P2 and A4P2.5 solutions were perfused with different rates from 0.5 to 5 μl/min for 5 min and the deposited fibers were examined by SEM (Fig. 3a). The deposition density was calculated by the total length of fiber in SEM pictures normalized by the picture area and the deposited time. Because the viscosity of C6P2 was less than that of A4P2.5 (14.1 Pa s *vs* 31.8 Pa s, Table s1), the collected fiber length of C6P2 was the double that of A4P2.5 (Fig. 3a). To confirm this result, the perfusion rate of 2 μl/min was applied to electrospin C6P2 or A4P2.5 to a circular cover slip with diameter of 16 mm. The collected fibers were weighed at different periods from 1 to 5 h. The results demonstrated that the collected C6P2 fibers were about the 1.6 times weight of the A4P2.5 fibers (Fig. 3b). Because the diameters of C6P2 fibers were thinner than that of A4P2.5 fibers (293 nm *vs* 322 nm) and the densities of C6P2 and A4P2.5 were almost identical (1.144 g/ml *vs* 1.140 g/ml), the relation between length and mass ratio should be 1.6, which is

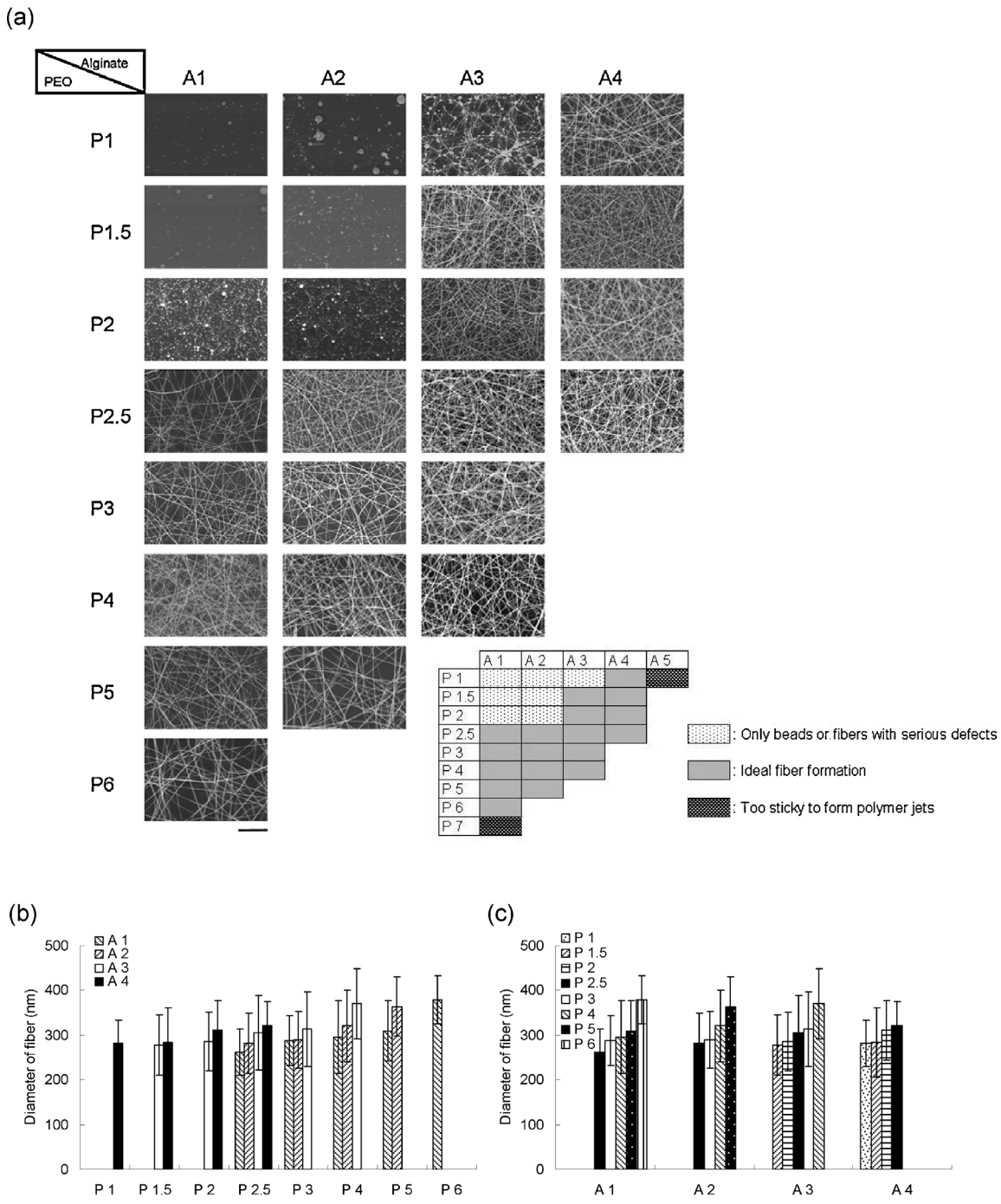

Fig. 2. The electrospinning of alginate/PEO fibers. (a) Polymer solutions with different concentrations of alginate and PEO were used for electrospinning, and the appropriate concentration range was also determined (scale bar = 10 μm). The diameters of nanofibers were compared using polymer solutions with different concentrations of (b) alginate and (c) PEO.

consistent to the mass ratio of nanofiber with equal perfusion rate.

$$\frac{M_C}{M_A} = \frac{\rho_C V_C}{\rho_A V_A} = \frac{\rho_C L_C D_C^2(\pi/4)}{\rho_A L_A D_A^2(\pi/4)}$$
$$= \frac{\rho_C}{\rho_A}\frac{L_C}{L_A}\left(\frac{D_C}{D_A}\right)^2 = \frac{1.144}{1.140} \times 2 \times \left(\frac{293}{322}\right)^2 \approx 1.6$$

The SEM and weight results suggested that the deposition rate of C6P2 fiber was the double that of A2P2.5 and the deposition rates were linearly correlated to the perfusion rates. Consequently, a dual-jet coelectrospinning device was developed to fabricate composite fibers (Supplementary Fig. s1). Different paired perfusion rates were applied to deposit C6P2 and A4P2.5 for producing composite chitosan/alginate fiber with different volumetric ratios (*i.e.* 80% C6P2, 50% C6P2, and 20% C6P2) (Table 1). These composite fibers were analyzed by XPS to determine both the signals of C1s and N1s. Because chitosan has amine groups while alginate does not, the nitrogen peaks should be proportional to the ratio of chitosan. The N/C ratio of pure C6P2 and pure A4P2.5 fibers were defined as 100% and 0%, respectively. The relative N/C ratios of composited nanofibers matched to their theoretical values, suggesting that the coelectrospinning system successfully prepared different

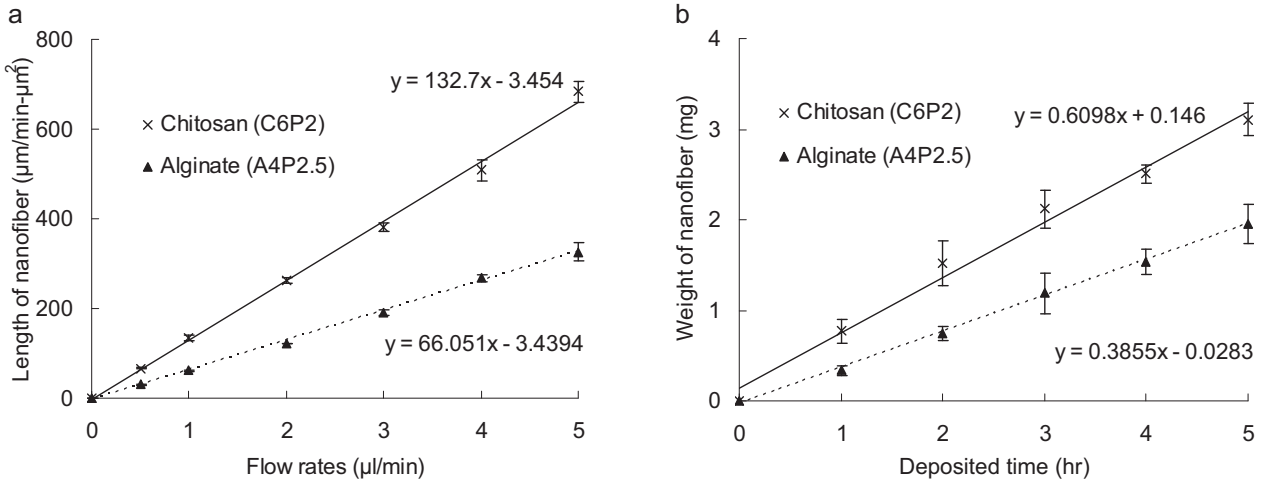

Fig. 3. Deposition rates of electrospun nanofibers. (a) C6P2 and A4P2.5 fibers were individually electrospun on glass cover slips for 5 min, and the surfaces fiber length was determine using SEM images, which was normalized by the area and time to determine the deposition density. (b) The perfusion rate of 2 μl/min was applied to electrospin C6P2 and A4P2.5, and the deposited fibers were weighed at different time points to determine the mass collection rates of these two fibers.

composition ratios of nanofibers (Fig. 4a). Furthermore, a fluorescent dye staining experiment was utilized to illustrate deposited nanofibers. Fluorescein and rhodamine B were used to stain C6P2 and A4P2.5 fibers, respectively. The green and red fibers were evenly distributed on surfaces with desired composition ratios, suggesting that this coelectrospinning can isotropically distribute two nanofibers with defined proportion (Fig. 4b). The SEM images illustrated that C6P2 and A4P2.5 fibers were evenly distributed on substrate surfaces (Fig. 4c). Because the average diameter of A4P2.5 was slightly larger than that of C6P2, higher ratio of A4P2.5 demonstrated thicker fibers.

3.4. Chemical properties of composite nanofibers

In our hypothesis, chemical properties of nanofibrous mats can be determined by their composition. Therefore, FTIR and water contact angle were applied to examine if this coelectrospinning method may modulate biomaterial surfaces.

For FTIR analysis, the spectrums of chitosan and alginate were similar because they are polysaccharides (Fig. 5a). For example, the peaks at 3400 and 1153 cm^{-1} contributed to the vibration of the OH group and the saccharide structures, respectively (Boonsongrit, Mueller, & Mitrevej, 2008). The absorption of PEO can be found at 1110 cm^{-1} for the C—O—C stretching and at 841 cm^{-1} for the stretching of the C—O—C and C—C (Ji et al., 2006). Because chitosan derived from chitin by deacetylation, there were two peaks of chitosan (C6P2) at 1560 and 1643 cm^{-1} attributed to its amine groups and un-deacetylated amide groups, respectively (Osman & Arof, 2003). On the other hand, the specific peak of alginate (A4P2.5) was at 1610 cm^{-1} due to the symmetric stretching vibration of the COO^- groups (Sarmento, Ferreira, Veiga, & Ribeiro, 2006). For the coelectrospun surfaces, the peaks at 1560 and 1643 cm^{-1} were proportional to the ratio of chitosan, and the absorption at 1610 cm^{-1} also increased with increasing alginate amounts. These results suggested that both chitosan and alginate fibers can be spun together by this dual-jet system, and their chemical properties can thus be controlled according to the composition ratios.

Table 1
The perfusion rates of polymer solutions for regulating the deposition ratios of C6P2 and A4P2.5 fibers.

	Perfusion rates (μl/min)		The composition ratios of C6P2 to A4P2.5
	C6P2	A4P2.5	
80% C6P2	2	1	8:2
50% C6P2	1	2	5:5
20% C6P2	0.5	4	2:8

In addition, water contact angle experiments were performed to determine the hydrophobicity of fiber deposited surfaces (Fig. 5b). Because alginate is a frequently used hydrogel material, A4P2.5 exhibited an extremely hydrophilic property that the water contact angle was only $19.5 \pm 1.0^\circ$. In contrast, C6P2 was more hydrophobic and its water contact angle was $60.3 \pm 1.2^\circ$. The coelectrospun fibers demonstrated hydrophobicity between A4P2.5 and C6P2 fibers, and the levels were proportional to the composition ratios, suggesting that the surface wettability can be regulated through deposited nanofibers.

3.5. Cell adhesion and viability of composite fibers

Previous FTIR and contact angle experiments demonstrated that coelectrospinning should be able to modify material surfaces by controlling the ratios of fiber deposition. It should be interesting to investigate if this surface modification may regulate cell adhesion and bioactivity. Therefore, C6P2, A4P2.5, and their composite fibers (80% C6P2, 50% C6P2, and 20% C6P2) were used to culture HEK-293T cells. Pure chitosan and alginate films were also applied as control groups. For cell morphology, there were no significant differences for all groups after 24 h of cell seeding that most of cells still unextended on material surfaces (Fig. 6a). At day 3, HEK-293T cells on chitosan films and C6P2 fibers demonstrated an epithelial-like morphology. In contrast, cell aggregation was found on alginate films and A4P2.5 fibers. The multicellular spheroids suggested that alginate surfaces were unfavorable for cell spreading. For composite fiber groups, cell morphologies were controlled by the fiber composition that cell shape gradually changed from epithelial-like cells to multicellular spheroids when alginate component was increased. This trend was more obvious at day 5.

The biocompatibility of nanofibers was evaluated by LDH and MTT assays to determine cell number and cell viability, respectively. Firstly, the comparisons of cells cultured either on films or fibers were performed to determine the effect of material format. There were more cells on fibers than that on films for both chitosan and alginate, and chitosan always demonstrated more cells than that on alginate surfaces at day 5 (Fig. 6b). The MTT assay at day 5

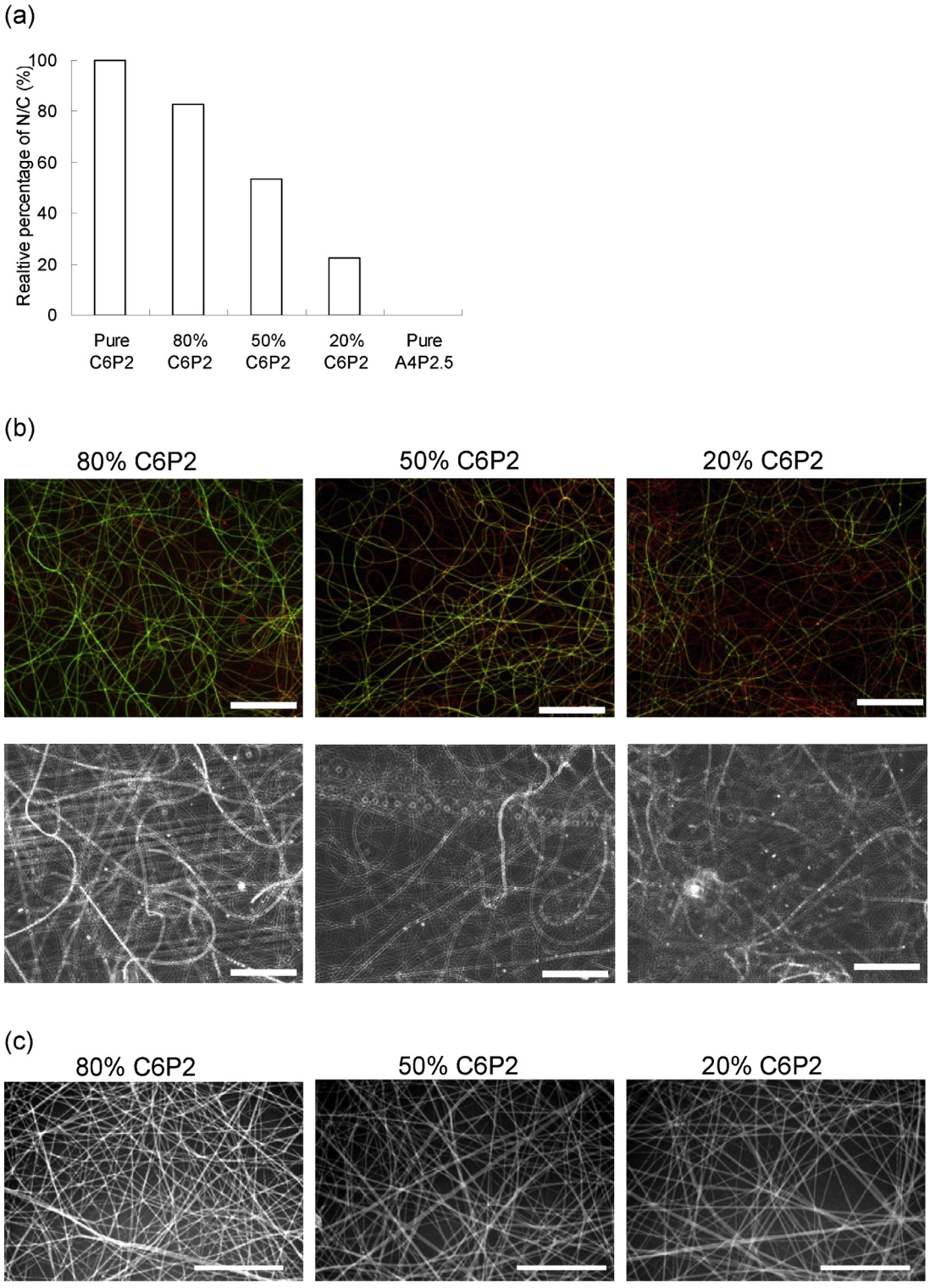

Fig. 4. The coelectrospinning of C6P2 and A4P2.5. (a) The element composition pure C6P2, A4P2.5, and their composite fibers were detected by XPS. The ratio of nitrogen to carbon signals were determined as N/C ratio, in which the pure C6P2 and pure A4P2.5 were defined as 100% and 0%, respectively. (b) Composite fibers were stained by fluorescent dyes to illustrate their composition ratio and distribution. The bright field images were also provided (green: C6P2; red: A4P2.5) (scale bar = 500 μm). (c) The SEM images of composite fibers (scale bar = 10 μm). (For interpretation of the references to color in this figure legend, the reader is referred to the web version of the article.)

revealed similar results that nanofibers had superior biocompatibilities to films (Fig. 6c).

For composite fibers, the promotion of cell proliferation was more obvious. The cell numbers on composite fibers were all greater than that on pure A4P2.5 fibers at both day 3 and day 5 (Fig. 6d). In addition, the results of 80% and 50% C6P2 groups were all higher than that of the pure C6P2 and A4P2.5 groups at day 3. Similar results were also demonstrated at the MTT results (Fig. 6e). These results suggested that composite fibers provided better environments than pure chitosan or alginate fibers, which were almost as good as the tissue culture polystyrene (TCPS) group and should be appropriate for cell adhesion and proliferation.

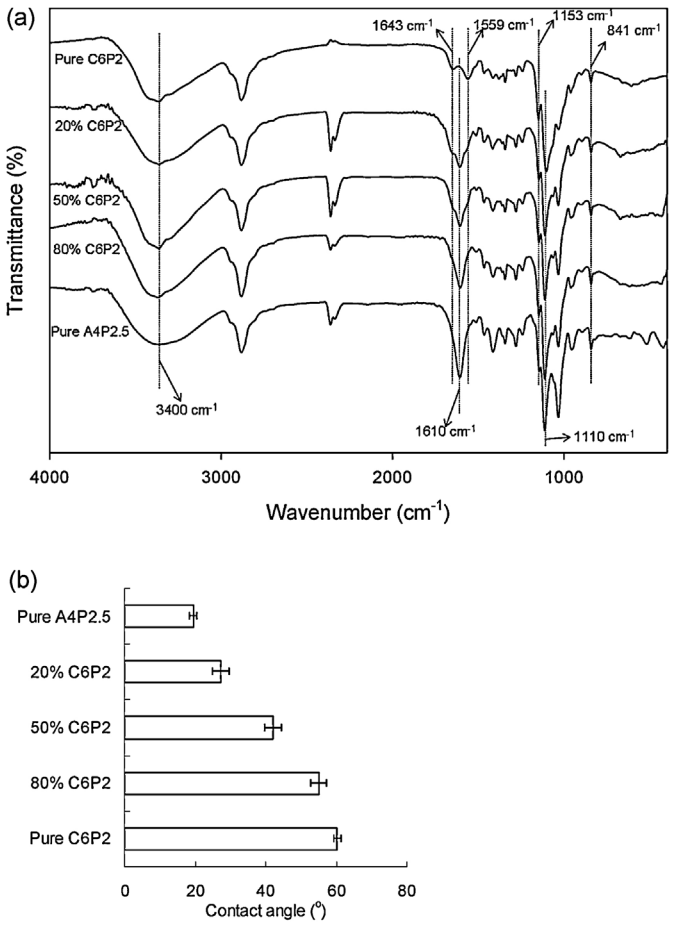

Fig. 5. The chemical properties of the composite fibers. (a) Chemical functional groups of electrospun fibers were examined by FTIR analysis. (b) The hydrophobicities of fiber mats were determined by water contact angle.

3.6. The degradation effect of composite nanofiber on cell adhesion and biocompatibility

In previous experiments, alginate fibers or films were all crosslinked in ethanol solutions with 2% of calcium chloride for 2 h to increase their integration because non-crosslinked alginate would be degraded in aqueous environment. To determine the effect of calcium ions on fiber stability, different concentrations of calcium chloride were applied to crosslink A4P2.5 nanofibers, and the residual fibers were weighed at different time points (Fig. 7a). Using 2% or more of calcium chloride for corsslinking can maintain more than 70% of the fiber mass, and the loss mass should be due to the release of PEO from fibers (Jeong, Krebs, Bonino, Khan, & Alsberg, 2010). In contrast, only 40% of fiber mass was maintained when fibers were crosslinked by 0.05% of $CaCl_2$ solution, suggesting that the insufficient calcium ion concentration resulted in 1/3 of fibers dissolved. For ethanol solution without calcium, all fibers were disappeared in 3 days. These results suggested that the stability of nanofibers can be controlled by simply using different concentrations of calcium ions during crosslinking.

From previous *in vitro* cell culture results of composite fibers, 50% C6P2 fibers demonstrated best biocompatibility. Therefore, we applied different concentrations of $CaCl_2$ solutions to crosslink 50% C6P2 fibers for studying their effect on cell adhesion and proliferation. Compared to the 2% $CaCl_2$ group that fibers were stable and the surfaces cell morphology was between C6P2 and A4P2.5 fibers, fibers crosslinked by 0.05% $CaCl_2$ demonstrated cell morphology between 50% C6P2 and 80% C6P2 that some round cells clumps and extended cells were both found at day 5 (Fig. 7b). In contrast, alginate fibers disappeared rapidly when the 0% of $CaCl_2$ solution was applied, and thus the surface cell morphology was similar to that on pure C6P2 fibers. These results suggested that the dissolved alginate fibers altered the composition of composite fibers and thus the cell morphology changed with time.

The LDH and MTT assays all indicated that there were no significant differences between nanofibers treated 2% and 0% of $CaCl_2$ solutions; however, using 0.05% of $CaCl_2$ solution for crosslinking demonstrated highest cell numbers and cell activity (Fig. 7c and d). These results should be due to that the disappearance of partial alginate fibers increased area for cell adhesion and thus the biocompatibility was improved.

4. Discussion

Because chitosan and alginate are two frequently used polysaccharides with different characteristics, the combination of these two materials should improve their properties. For example, scaffolds fabricated by the blending of chitosan and alginate have been proved to promote mechanical strength and increase cell proliferation (Li, Ramay, Hauch, Xiao, & Zhang, 2005). In addition, due to the attraction between carboxyl groups of alginate and amino groups of chitosan, their combination can stabilize materials structure at wide range of pH changes (Deng et al., 2010; Yan, Khor, & Lim, 2000). For electrospinning, because blending of alginate and chitosan may form a hydrogel due to complexation, it may inhibit polymer solution perfusion through needle (Lim, Liao, & Leong, 2006). Therefore, a dual applicator tip needle has been applied to mix chitosan and alginate solutions immediately before spinning from needle,

which can *in situ* complex chitosan–alginate to prepare nanofibers (Jeong et al., 2011). However, the compatibility of alginate and chitosan solutions were restricted by different parameters, such as the molecular weight, pH, and thus the blending ratio was limit (Gaserod, Smidsrod, & Skjak-Braek, 1998). Therefore, we developed a coelectrospinning method using dual jet system to overcome these problems. Chitosan and alginate fibers were solely spun using two independent power supplies. Because the perfusion rates of polymer solution during electrospinning can be controlled to regulate the deposition ratios, different compositions of nanofibers can be collected arbitrarily.

Before coelectrospinning process, the morphology and deposition rate of nanofibers were investigated independently. The existence of PEO was necessary to increase the entanglement of polymer chains. Higher concentrations of polymer solutions resulted in higher viscosities, which resulted in spun fibers with larger diameters. By systemically examination, appropriate ranges of polymer composition were thus determined.

The C6P2 and A4P2.5 solutions were applied for coelectrospinning. The deposition rates were linearly corresponding to the perfusion rates. When the perfusion rates were identical, the deposition rates of C6P2 was almost the double that of A4P2.5. Therefore, different pairs of perfusion rates were applied to prepare composite nanofibers. The fluorescent staining and XPS results suggested that the composition of fibers were according to the design. In addition, the compositions of functional groups and the hydrophobicities of deposited surfaces were also proportional to the ratios of fibers, suggesting that this method can modulate biomaterial to optimize surfaces properties. Upon our knowledge, it should be the first report of controlling the composition ratios of multiple electrospun nanofibers by the perfusion rates of polymer solutions. Compared to conventional methods using blended polymer solutions for electrospinning, this easy and straightforward method can delicately modify surfaces properties for different applications.

The cell culture results demonstrated that nanofiber forms of materials performed better biocompatibilities than that as bulk ones. Similar results have been reported that nanofiber of chitosan can promote the attachment of osteoblasts, chondrocytes, and hepatocytes, which not only maintains characteristic cell morphologies but also improves cell viabilities (Bhattarai et al., 2005; Chu, Shi, Feng, Gu, & Ding, 2009). This should be due to that nanofibrous structure is more close to the extracellular matrix environment and provides more area for cell adhesion and growth.

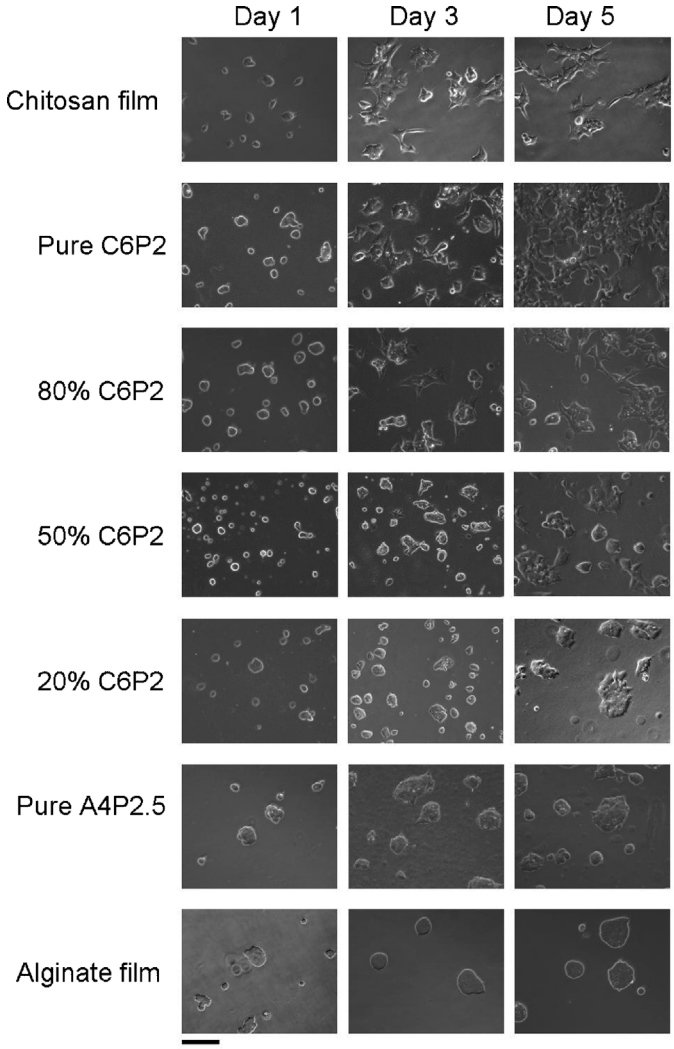

Fig. 6. The effect of nanofiber composition on cell morphology and biocompatibility. (a) Different nanofibers were used to culture HEK-293T cells, and the surface cell morphologies were examined by inverted microscopy. Chitosan and alginate film surfaces were applied as the control groups (scale bar = 100 μm). To evaluate the promotion of biocompatibility by electrospinning, HEK-293T cells were cultured on films or fibers of chitosan or alginate, and the total cell numbers and cell activity of were evaluated by (b) LDH and (c) MTT assay, respectively ($^{*}p < 0.05$ and $^{**}p < 0.01$). The effect of nanofiber composition on biocompatibility was also determined by the (d) LDH and (e) MTT results ($^{*}p < 0.05$ compared with A4P2.5, $^{**}p < 0.01$ compared with A4P2.5, $^{\#}p < 0.05$ compared with C6P2, and $^{\#\#}p < 0.01$ compared with C6P2).

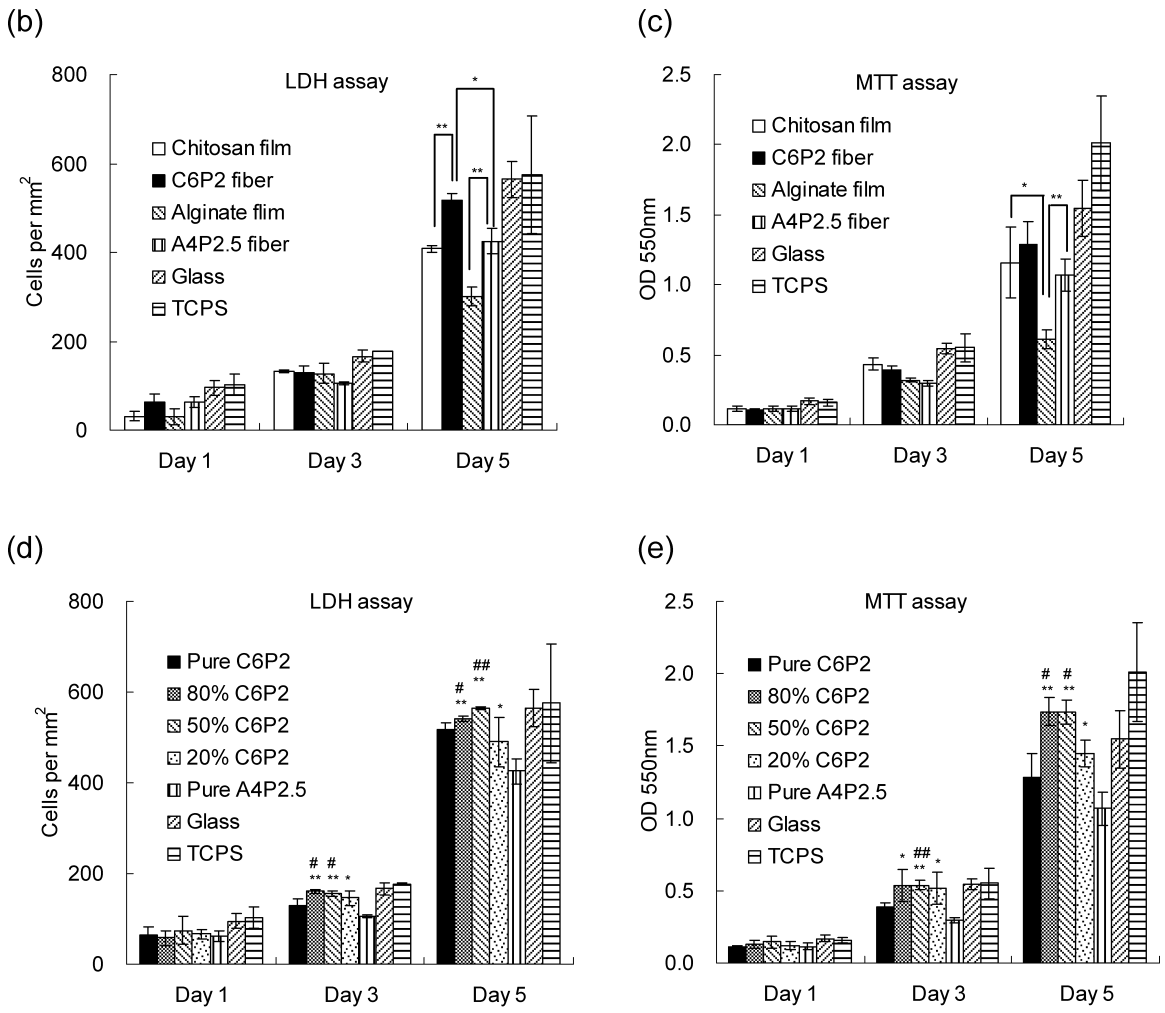

Fig. 6. (*continued*).

Furthermore, compared to pure C6P2 and A4P2.5 fibers, composite fibers demonstrated better biocompatibilities. It should be due to that the coexistance of chitosan and alginate provided their own specific functions to refine surface properties. Alginate is an extremely hydrophilic material, and thus can increase water content to create a hydrate environment for cell growth. However, hydrophilic material is not attractive to protein adsorption, and thus ECM constituent such as fibronectin or collagen are hard to be maintained on alginate surfaces, which inhibits cell adhesion (Smetana, 1993). In addition, negative charged cells surfaces are not favor to contact to anionic alginate fibers. Chitosan demonstrates different properties to alginate due to its positive charges and relative hydrophobic surfaces that are more favorable for cell adhesion and protein adsorption. Therefore, our coelectrospinning method can deposit both chitosan and alginate fibers on the same surfaces to modulate their properties, and our results suggested that 50% C6P2 fibers should provide appropriate environments for cells adhesion and proliferation.

Although scaffolds may provide mechanical support for tissue engineering application, undegradable scaffolds may occupy spaces to inhibit the ingrowths of newly formed tissues. Therefore, the degradation rate of biomaterial is critical. Gamma irradiation has been used to treat high molecular weight of alginate, which can produce different polymer chain length and structure for controlling the degradation rates (Alsberg et al., 2003). Because alginate can be stabilized by ionic crosslinking, different concentrations of calcium ions were applied in this study, and our results demonstrated that 2% or more of calcium chloride solutions can stably maintain alginate fibers that the mass loss was mainly due to the release of PEO. When the calcium ions concentration was decreased to 0.05%, low concentrations of calcium ions made incomplete crosslinking and partial alginate fibers were thus degraded. In contrast, the release of PEO from C6P2 fibers was also occurred in aqueous environment, whereas the ratio of mass loss and the integrity of fibers were independent of the calcium ions (data not shown). The cell morphologies were thus affected by the crosslinking levels of alginate. The cell shape on 50% C6P2 was more close to that on 80% C6P2 when the fibers were crosslinked by 0.05% $CaCl_2$, suggesting that the fiber composition was changed with time. In addition, alginate fibers without calcium crosslinking were degraded quickly in 3 days, and thus cells on 50% C6P2 was more close to that on pure C6P2 at day 5 due to disappearance of alginate fibers. This controllable degradation also may affect cell viability that the partial degradation of alginate fiber using 0.05% $CaCl_2$ may promote biocompatibility. Compared to the stable fibers crosslinked by 2% of $CaCl_2$, 0.05% $CaCl_2$ caused the fiber composition varied with time. Some alginate fibers degraded and more space was available for cell ingrowth. On the other hand, non-crosslinking resulted in quick degradation of alginate fibers that the surfaces properties were eventually became pure chitosan only. These results suggested that the cell morphology and biocompatibility can be dynamically controlled through the degradation of nanofibers. Through these regulations, biomaterials can be delicately optimized to fit various applications.

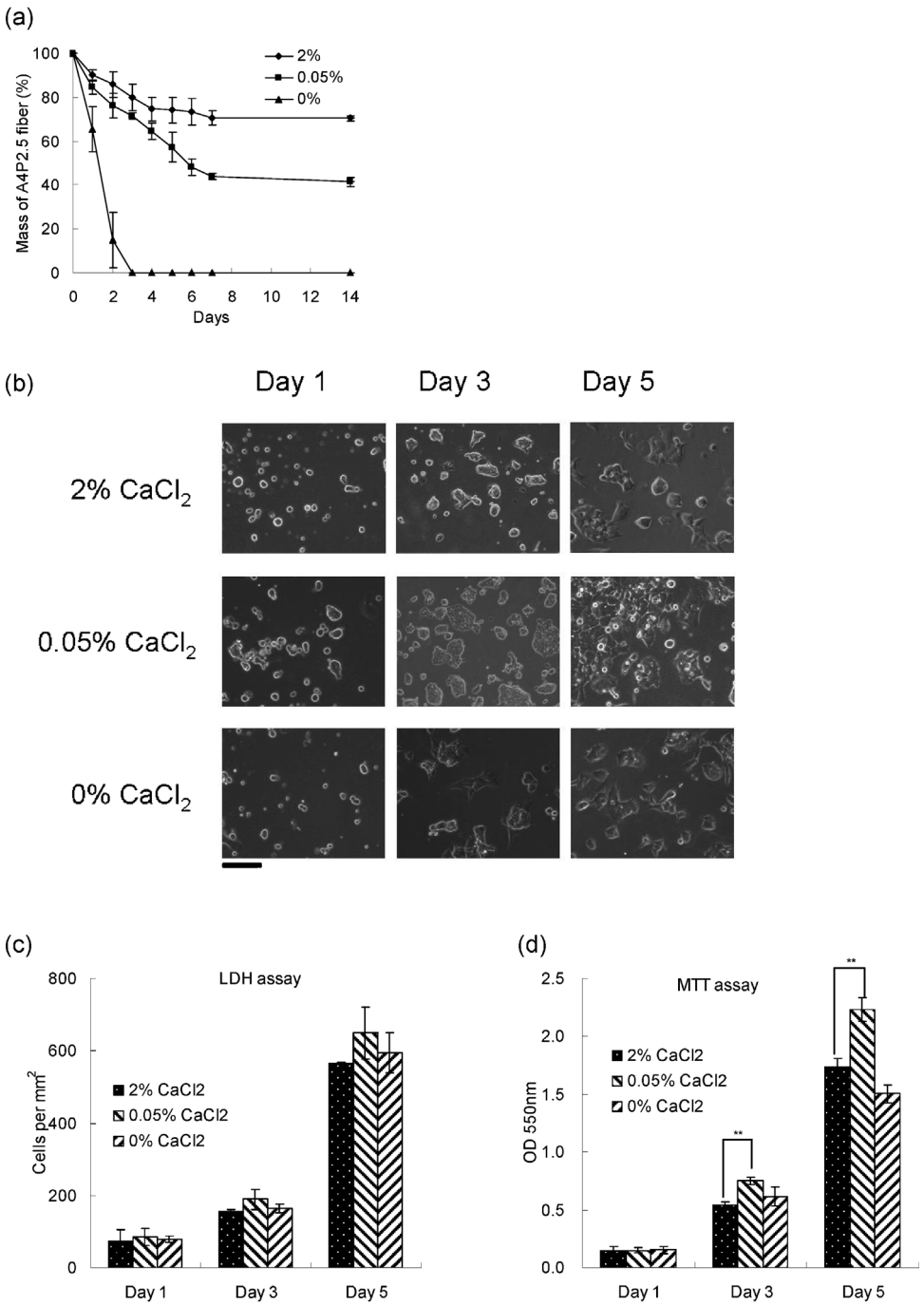

Fig. 7. The effect of nanofiber degradation on cell morphology and biocompatibility. A4P2.5 fibers were crosslinked by different concentrations of calcium chloride solutions for 2 h before immersing to PBS. These fibers were weighed to determine the residual fibers. 50% C6P2 fibers were crosslinked by different concentrations of calcium chloride solutions for 2 h before culturing HEK-293T cells. (b) The surface cell morphologies were examined by inverted microscopy (scale bar = 100 μm). The effect of fiber degradation on biocompatibility were compared by (c) LDH and (d) MTT assay ($^{*}p < 0.05$ and $^{**}p < 0.01$).

5. Conclusions

In this study, chitosan and alginate nanofibers are successfully fabricated using electrospinning technique. The addition of PEO increases the viscosity of polymer solution to facilitate the fiber formation. The deposition of nanofibers can be regulated through adjusting the perfusion rates of polymer solutions during electrospinning. Therefore, a dual jet system is developed for coelectrospinning that the composition of fibers can be simply controlled to fabricate fibrous mats with different surface properties. The *in vitro* cell culture reveals that the shapes of adhered cells highly depend on the composition of nanofibers. In addition, the composite fibers demonstrate better biocompatibility than that on pure fibers, suggesting that the surface properties can be finely tuned to create an optimal environment. By controlling the crosslinking process, partial of alginate fibers degrades with time to alter the fiber composition. Therefore, our developed coelectrospinning system can control the fiber ratio not only by the composition of fiber deposition but also through the changing of degradation rates, which should provide an attractive approach to dynamically modulate surfaces properties and may be beneficial to tissue engineering applications.

Acknowledgements

This research was supported by the grant of NSC 101-2221-E-008-090-MY2 from the National Science Council of Taiwan, and 100CGH-NCU-A2 from the National Central University and Cathy General Hospital Joint Research Center.

Appendix A. Supplementary data

Supplementary data associated with this article can be found, in the online version, at http://dx.doi.org/10.1016/j.carbpol.2013.02.083.

References

Alsberg, E., Kong, H. J., Hirano, Y., Smith, M. K., Albeiruti, A., & Mooney, D. J. (2003). Regulating bone formation via controlled scaffold degradation. *Journal of Dental Research*, *82*(11), 903–908.

Baker, B. M., Gee, A. O., Metter, R. B., Nathan, A. S., Marklein, R. A., Burdick, J. A., et al. (2008). The potential to improve cell infiltration in composite fiber-aligned electrospun scaffolds by the selective removal of sacrificial fibers. *Biomaterials*, *29*(15), 2348–2358.

Bhattarai, N., Edmondson, D., Veiseh, O., Matsen, F. A., & Zhang, M. (2005). Electrospun chitosan-based nanofibers and their cellular compatibility. *Biomaterials*, *26*(31), 6176–6184.

Bhattarai, N., Li, Z. S., Edmondson, D., & Zhang, M. Q. (2006). Alginate-based nanofibrous scaffolds: Structural, mechanical, and biological properties. *Advanced Materials*, *18*(11), 1463.

Boonsongrit, Y., Mueller, B. W., & Mitrevej, A. (2008). Characterization of drug–chitosan interaction by H-1 NMR, FTIR and isothermal titration calorimetry. *European Journal of Pharmaceutics and Biopharmaceutics*, *69*(1), 388–395.

Chang, J. J., Lee, Y. H., Wu, M. H., Yang, M. C., & Chien, C. T. (2012). Preparation of electrospun alginate fibers with chitosan sheath. *Carbohydrate Polymers*, *87*(3), 2357–2361.

Chu, X. H., Shi, X. L., Feng, Z. Q., Gu, Z. Z., & Ding, Y. T. (2009). Chitosan nanofiber scaffold enhances hepatocyte adhesion and function. *Biotechnology Letters*, *31*(3), 347–352.

Dar, A., Shachar, M., Leor, J., & Cohen, S. (2002). Optimization of cardiac cell seeding and distribution in 3D porous alginate scaffolds. *Biotechnology and Bioengineering*, *80*(3), 305–312.

Deng, H. B., Wang, X. Y., Liu, P., Ding, B., Du, Y. M., Li, G. X., et al. (2011). Enhanced bacterial inhibition activity of layer-by-layer structured polysaccharide film-coated cellulose nanofibrous mats via addition of layered silicate. *Carbohydrate Polymers*, *83*(1), 239–245.

Deng, H. B., Zhou, X., Wang, X. Y., Zhang, C. Y., Ding, B., Zhang, Q. H., et al. (2010). Layer-by-layer structured polysaccharides film-coated cellulose nanofibrous mats for cell culture. *Carbohydrate Polymers*, *80*(2), 474–479.

Duan, B., Dong, C., Yuan, X., & Yao, K. (2004). Electrospinning of chitosan solutions in acetic acid with poly(ethylene oxide). *Journal of Biomaterials Science, Polymer Edition*, *15*(6), 797–811.

Gaserod, O., Smidsrod, O., & Skjak-Braek, G. (1998). Microcapsules of alginate–chitosan. I. A quantitative study of the interaction between alginate and chitosan. *Biomaterials*, *19*(20), 1815–1825.

Geng, X. Y., Kwon, O. H., & Jang, J. H. (2005). Electrospinning of chitosan dissolved in concentrated acetic acid solution. *Biomaterials*, *26*(27), 5427–5432.

Jeon, O., Powell, C., Ahmed, S. M., & Alsberg, E. (2010). Biodegradable, photocrosslinked alginate hydrogels with independently tailorable physical properties and cell adhesivity. *Tissue Engineering A*, *16*(9), 2915–2925.

Jeong, S. I., Krebs, M. D., Bonino, C. A., Khan, S. A., & Alsberg, E. (2010). Electrospun alginate nanofibers with controlled cell adhesion for tissue engineering. *Macromolecular Bioscience*, *10*(8), 934–943.

Jeong, S. I., Krebs, M. D., Bonino, C. A., Samorezov, J. E., Khan, S. A., & Alsberg, E. (2011). Electrospun chitosan–alginate nanofibers with in situ polyelectrolyte complexation for use as tissue engineering scaffolds. *Tissue Engineering A*, *17*(1–2), 59–70.

Ji, Y., Ghosh, K., Shu, X. Z., Li, B. Q., Sokolov, J. C., Prestwich, G. D., et al. (2006). Electrospun three-dimensional hyaluronic acid nanofibrous scaffolds. *Biomaterials*, *27*(20), 3782–3792.

Karageorgiou, V., & Kaplan, D. (2005). Porosity of 3D biomaterial scaffolds and osteogenesis. *Biomaterials*, *26*(27), 5474–5491.

Li, Z. S., Ramay, H. R., Hauch, K. D., Xiao, D. M., & Zhang, M. Q. (2005). Chitosan–alginate hybrid scaffolds for bone tissue engineering. *Biomaterials*, *26*(18), 3919–3928.

Lim, S. H., Liao, I. C., & Leong, K. W. (2006). Nonviral gene delivery from nonwoven fibrous scaffolds fabricated by interfacial complexation of polyelectrolytes. *Molecular Therapy*, *13*(6), 1163–1172.

Lu, J. W., Zhu, Y. L., Guo, Z. X., Hu, P., & Yu, J. (2006). Electrospinning of sodium alginate with poly(ethylene oxide). *Polymer*, *47*(23), 8026–8031.

Majima, T., Funakosi, T., Iwasaki, N., Yamane, S. T., Harada, K., Nonaka, S., et al. (2005). Alginate and chitosan polyion complex hybrid fibers for scaffolds in ligament and tendon tissue engineering. *Journal of Orthopaedic Science*, *10*(3), 302–307.

Min, B. M., Lee, S. W., Lim, J. N., You, Y., Lee, T. S., Kang, P. H., et al. (2004). Chitin and chitosan nanofibers: Electrospinning of chitin and deacetylation of chitin nanofibers. *Polymer*, *45*(21), 7137–7142.

Nam, J., Huang, Y., Agarwal, S., & Lannutti, J. (2007). Improved cellular infiltration in electrospun fiber via engineered porosity. *Tissue Engineering*, *13*(9), 2249–2257.

Osman, Z., & Arof, A. K. (2003). FTIR studies of chitosan acetate based polymer electrolytes. *Electrochimica Acta*, *48*(8), 993–999.

Ritcharoen, W., Supaphol, P., & Pavasant, P. (2008). Development of polyelectrolyte multilayer-coated electrospun cellulose acetate fiber mat as composite membranes. *European Polymer Journal*, *44*(12), 3963–3968.

Rnjak-Kovacina, J., Wise, S. G., Li, Z., Maitz, P. K. M., Young, C. J., Wang, Y. W., et al. (2011). Tailoring the porosity and pore size of electrospun synthetic human elastin scaffolds for dermal tissue engineering. *Biomaterials*, *32*(28), 6729–6736.

Rowley, J. A., Madlambayan, G., & Mooney, D. J. (1999). Alginate hydrogels as synthetic extracellular matrix materials. *Biomaterials*, *20*(1), 45–53.

Sarmento, B., Ferreira, D., Veiga, F., & Ribeiro, A. (2006). Characterization of insulin-loaded alginate nanoparticles produced by ionotropic pre-gelation through DSC and FTIR studies. *Carbohydrate Polymers*, *66*(1), 1–7.

Shao, X. X., & Hunter, C. J. (2007). Developing an alginate/chitosan hybrid fiber scaffold for annulus fibrosis cells. *Journal of Biomedical Materials Research Part A*, *82A*(3), 701–710.

Sill, T. J., & von Recum, H. A. (2008). Electro spinning: Applications in drug delivery and tissue engineering. *Biomaterials*, *29*(13), 1989–2006.

Smetana, K. (1993). Cell biology of hydrogels. *Biomaterials*, *14*(14), 1046–1050.

Soliman, S., Pagliari, S., Rinaldi, A., Forte, G., Fiaccavento, R., Pagliari, F., et al. (2010). Multiscale three-dimensional scaffolds for soft tissue engineering via multimodal electrospinning. *Acta Biomaterialia*, *6*(4), 1227–1237.

Telemeco, T. A., Ayres, C., Bowlin, G. L., Wnek, G. E., Boland, E. D., Cohen, N., et al. (2005). Regulation of cellular infiltration into tissue engineering scaffolds composed of submicron diameter fibrils produced by electrospinning. *Acta Biomaterialia*, *1*(4), 377–385.

Vaquette, C., & Cooper-White, J. J. (2011). Increasing electrospun scaffold pore size with tailored collectors for improved cell penetration. *Acta Biomaterialia*, *7*(6), 2544–2557.

Woodfield, T. B. F., Van Blitterswijk, C. A., De Wijn, J., Sims, T. J., Hollander, A. P., & Riesle, J. (2005). Polymer scaffolds fabricated with pore-size gradients as a model for studying the zonal organization within tissue-engineered cartilage constructs. *Tissue Engineering*, *11*(9–10), 1297–1311.

Yan, X. L., Khor, E., & Lim, L. Y. (2000). PEC films prepared from chitosan–alginate coacervates. *Chemical and Pharmaceutical Bulletin*, *48*(7), 941–946.